

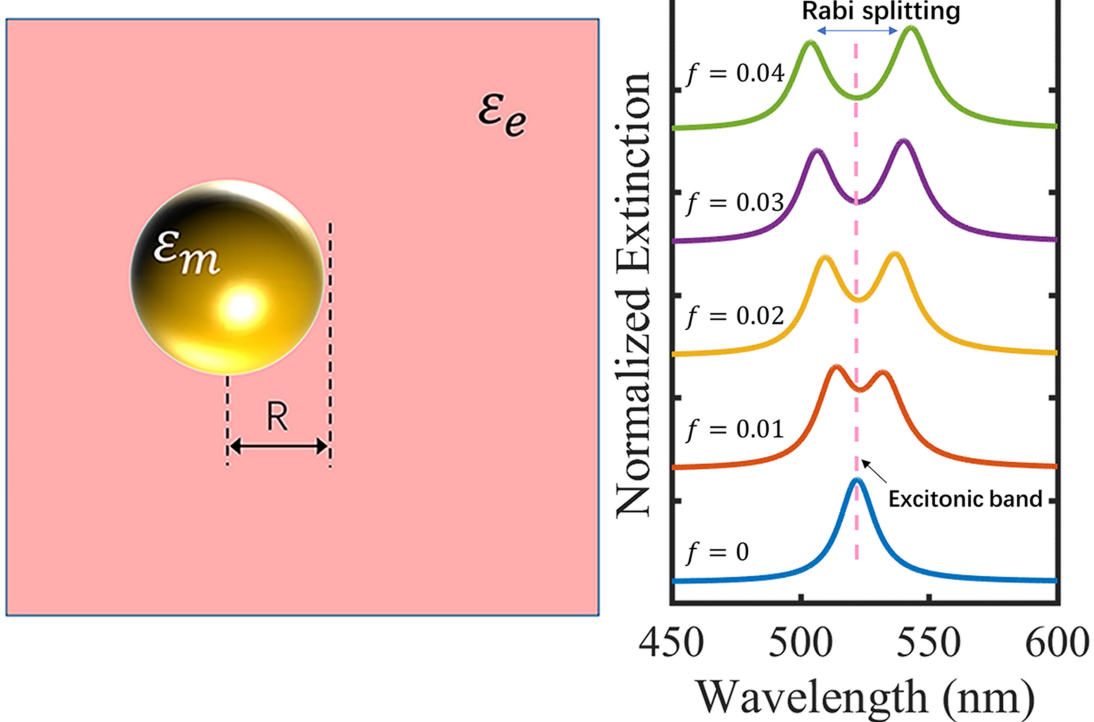
A Semiclassical Model for Plasmon-Exciton Interaction From Weak to Strong Coupling Regime

Volume 13, Number 3, June 2021

Fan Wu

Rongzhen Jiao

Li Yu



DOI: 10.1109/JPHOT.2021.3070061

A Semiclassical Model for Plasmon-Exciton Interaction From Weak to Strong Coupling Regime

Fan Wu , Rongzhen Jiao, and Li Yu 

School of Science, Beijing University of Posts and Telecommunications, Beijing 100876, China

DOI:10.1109/JPHOT2021.3070061

This work is licensed under a Creative Commons Attribution-NonCommercial-NoDerivatives 4.0 License. For more information, see <https://creativecommons.org/licenses/by-nc-nd/4.0/>

Manuscript received January 19, 2021; revised March 16, 2021; accepted March 29, 2021. Date of publication March 31, 2021; date of current version April 21, 2021. This work was supported in part by the National Key R&D Program of China under Grant 2016YFA0301300, in part by the Fundamental Research Funds for the Central Universities, in part by the National Natural Science Foundation of China under Grant 11574035, and in part by the Fund of State Key Laboratory of Information Photonics and Optical Communications (Beijing University of Posts and Telecommunications), PR China. Corresponding author: Li Yu (e-mail: yuliyuli@bupt.edu.cn).

This article has supplementary downloadable material available at <https://doi.org/10.1109/JPHOT.2021.3070061>, provided by the authors.

Abstract: Exploitation of strong light-matter interactions in plasmonic systems is vital for both fundamental studies and the development of new applications, which enables exceptional physical phenomena and promotes potential applications in nanophotonics, information communication, and quantum information processing. Here, we present an analytic model of the interaction between localized surface plasmon resonances and excitons, where a semiclassical method is utilized. Two kinds of metal nanoparticles (nanosphere and nanoellipsoid) are considered in our study. We derive the relations between the plasmon-exciton coupling strength and the geometry and material parameters of the coupled systems when the nanoparticles are put in an excitonic medium, which give an important guide to achieve strong plasmon-exciton coupling. Rabi splittings and anticrossing behavior are also demonstrated in the calculated extinction spectra. Furthermore, we propose an analytic model to describe the strong coupling between excitons and plasmon in a core-shell nanorod structure which is widely used in experiments. Our study provides a simple yet rigorous prescription to both analyze and design plexcitonic systems aiming at strong light-matter interactions.

Index Terms: Metal nanoparticles, localized surface plasmon resonances, plasmon-exciton interaction, strong coupling.

1. Introduction

Strong light-matter interactions not only are significant for fundamental quantum optics but also are beneficial for exploring advanced quantum devices. The plasmonic nanocavities can confine light to the sub-wavelength scale giving an ultralow mode volume, and possess the merits of achieving strong light-matter interactions at room temperature [1]–[4]. Thus, the plasmon-exciton coupling has attracted great interest in recent years [5]–[11]. When a surface plasmon mode strongly interacts with excitonic material, new plasmon-exciton hybrid states called plexcitons emerge [12]–[14], which have significant applications such as Bose-Einstein condensation, [15] low threshold laser [16], and quantum information processing [17]. Plexcitons are mainly characterized

by Rabi splittings in spectra and avoided crossing behavior in dispersion diagrams of the coupled systems. To date, strong plasmon-exciton coupling has been experimentally achieved in many configurations, including thin metal films with excitonic layers [18], [19], nanoparticles coated with excitonic materials [1], [20], and the nanogap between plasmonic structures filled with molecules or quantum dots [21]–[26]. Rabi splittings in different spectra such as scattering spectra [14], [21], extinction spectra [27], photoluminescence spectra [12], [28], and circular dichroism spectrum [29] also have been demonstrated.

In order to achieve strong plasmon-exciton coupling, the characteristics of the plasmonic nanocavities are crucial. The material and geometrical requirements for specific plasmonic nanostructures are expected to be known when designing the plexcitonic structures. However, most of the previous studies of plasmon-exciton coupling relied on purely phenomenological models of classical coupled oscillators [7], [14], [30], [31]. In these phenomenological models, the magnitude of the coupling strength is introduced as a free parameter not explicitly connected to the material or geometrical properties of the coupled system. And in some quantum theories, a general relationship between coupling energy g and the effective cavity volume V is given by $g \propto 1/\sqrt{V}$ [1], [24], [26], yet one cannot directly obtain geometric and material requirements for the plasmonic structures to achieve strong coupling as well. In order to clarify the influence of the geometry and the material parameters of the coupled system on the light-matter interaction, herein we develop an analytical model based on classical electromagnetic analysis of metal nanoparticles and a semiclassical description of the electronic transitions related to the excitonic material to solve plasmon-exciton coupling. The following three configurations are considered: 1) a metal nanosphere in excitonic medium, 2) a metal nanoellipsoid in excitonic medium, and 3) a metal nanoellipsoid coated with an excitonic layer. The rigorous analytical relations between the coupling interaction strength and the material and geometrical parameters are given. In configuration 1), we investigate the specific material requirements of the metal nanosphere and the excitonic medium for strong coupling. Rabi splitting is demonstrated in the extinction spectra. In configuration 2), we discuss the influence of the aspect ratios of the metal nanoellipsoid on the coupling strength. We also track anticrossing behavior by adjusting the surface plasmon resonance across the exciton absorption band. At last, we investigate a practical configuration: a metal ellipsoid coated with an excitonic layer, which could be used to describe core-shell nanorod plexcitonic systems widely used in experiments.[1], [12] The relation of the layer thickness and Rabi splitting is obtained. Our results provide a useful guide in designing plexcitonic systems and have potential applications in quantum information processing, bio-sensing, and individual nanoscale optical devices.

2. Metal Nanosphere in Excitonic Medium

Let's start with the simplest case, a metal nanosphere put in an excitonic medium. Metal nanospheres are the most basic plasmonic nanoparticles, which support localized surface plasmon resonance. They are widely used in the research of nano-optics due to their theoretical simplicity and experimental accessibility. In spite of this, when it comes to the metal nanosphere coupling with excitonic material, the strict analytic relationship between the plasmon-exciton interaction strength and the material parameters of the coupled systems has not been given. In this section, we will discuss this issue in detail.

Fig. 1(a) shows a metal nanosphere in a uniform and infinite excitonic medium. According to a classical electromagnetic analysis (see the Supplementary Information, Section S1), the polarizability of the nanosphere is given by:

$$\alpha_1 = 4\pi R^3 \frac{\varepsilon_m - \varepsilon_e}{\varepsilon_m + 2\varepsilon_e}. \quad (1)$$

The permittivity of the excitonic material ε_e is described by a Lorentzian model: $\varepsilon_e = \varepsilon_\infty - f\omega_0^2/(\omega^2 - \omega_0^2 + i\Gamma_0\omega)$, where ε_∞ is a parameter describing the permittivity at $f = 0$. Γ_0 is the line width. f is the reduced oscillator strength, which is proportional to N/V , the number density of oscillators[9]. we can consider the excitonic medium as a polymer background containing dye

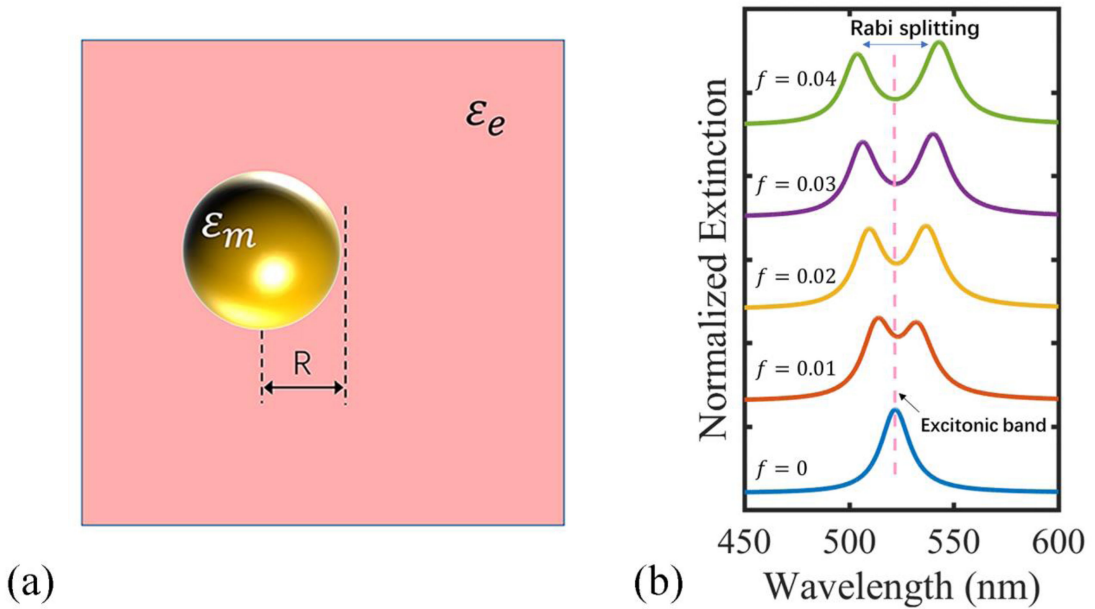


Fig. 1. (a) Schematic diagram of a metal nanosphere surrounded by excitonic material. ϵ_m is the permittivity of the metal and ϵ_e is the permittivity of the excitonic material. R is the radius of the nanosphere. (b) Extinction spectra of Au nanospheres in excitonic material with different oscillator strength f .

molecules with a suitable optical absorption or consider the excitonic medium as quantum dots dispersed in solutions, then f can be adjusted by the dye molecules or quantum dots concentration. The permittivity of the metal is described by a Drude model [32]: $\epsilon_m = \epsilon_\infty^D - \omega_p^2 / (\omega^2 + i\omega\Gamma_m)$. ω_p is the plasma frequency of the free electron gas, and ϵ_∞^D is a dielectric constant that describes the residual polarization effect due to the positive background of the ion cores. For small metal spheres, the absorption is much stronger than scattering and dominates the extinction. The extinction cross section is given by $C_{ex_1} \approx C_{abs} = klm[\alpha_1]$ (see the Supplementary Information, Section S5). We can calculate the extinction cross section of the metal nanosphere by substituting the expression of ϵ_m and ϵ_e into (1). Fig. 1(b) shows the extinction spectra of a Au nanosphere in excitonic media with different oscillator strength f . ϵ_∞ is set to 1.77 (water). The resonance frequency ω_0 is set to 2.36 eV, Γ_0 is set to 50 meV which is a typical linewidth of J-aggregates [33]. The radius of the nanosphere is set to 15 nm. In the case of $f = 0$, ϵ_e is a real number, and the extinction spectrum exhibits an uncoupled surface plasmon resonance. Then, as f increases, Rabi splitting, a characteristic strong coupling phenomenon, occurs in the extinction spectra and becomes larger as f increases. The two generated resonance peaks correspond to the two energy branches of the hybrid modes branches, the upper (UB) and lower (LB) branches.

Next, by further simplifying the analysis results, the conditions required to observe the Rabi splitting and the correlation between coupling strength and material parameters are discussed. Here, we define the localized surface plasmon resonance frequency as ω_m . ω_m satisfies the following equation: $Re[\epsilon_m + 2\epsilon_e] = 0$ in the uncoupled case ($f = 0$), which leads to $\omega_m^2 = \omega_p^2 / (\epsilon_\infty^D + 2\epsilon_\infty)$. We assume that $\omega \approx \omega_0 \approx \omega_m$. Then, the extinction cross section can be given by $C_{ex_1} \propto Im[1/(\omega - \tilde{\omega}_{1-}) - 1/(\omega - \tilde{\omega}_{1+})]$ (see the Supplementary Information, Section S4). Therefore, two resonance branches corresponding to $\tilde{\omega}_{1\pm}$ will appear in the extinction spectrum. $\tilde{\omega}_{1\pm}$ are expressed as:

$$\tilde{\omega}_{1\pm} = \frac{\tilde{\omega}_m + \tilde{\omega}_0}{2} \pm \sqrt{\left(\frac{\tilde{\omega}_m - \tilde{\omega}_0}{2}\right)^2 + G_1^2}. \quad (2)$$

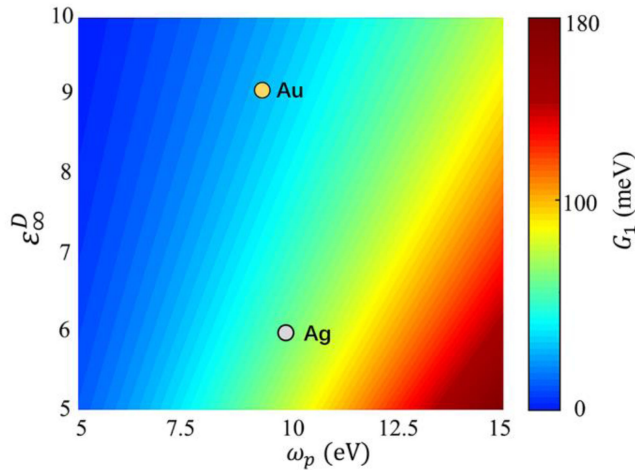


Fig. 2. Evolution of coupling constant vs the plasma frequency ω_p of the metal and the value of ϵ_{∞}^D . The golden and silver dots correspond to the Au and Ag nanosphere, respectively.

Here, we introduce the following complex frequencies $\tilde{\omega}_0 = \omega_0 - i\Gamma_0/2$ and $\tilde{\omega}_m = \omega_m - i\Gamma_m/2$. G_1 is given by:

$$G_1^2 = \frac{f\omega_p^2}{2(\epsilon_{\infty}^D + 2\epsilon_{\infty})^2}. \quad (3)$$

The parameter G_1 determines the magnitude of the resonance energy difference between the UB and LB when the detuning between plasmons and exciton is close to zero ($\omega_m \approx \omega_0$). Thus, we defined the plasmon-exciton coupling constant as G_1 . According to (3), the coupling strength has no dependence on the magnitude of the electric near-field around the nanosphere when they are homogeneously coated with the excitonic material. Instead, the coupling strength depends on the material properties of the excitonic material and the metal. It is easy to find a linear relationship between f and the square of Rabi splitting. As f increases, the interaction between plasmons and excitons becomes stronger, leading to a larger Rabi splitting. This is consistent with the changing trend shown in Fig. 2. Equation (3) also shows that G_1^2 increases with decreasing the value of ϵ_{∞} , indicating that strong coupling can be more easily observed for excitonic materials with a low background permittivity. Let us now examine in more detail the dependence of G_1 on the material properties of the metal sphere ($\epsilon_{\infty}^D, \omega_p$). In this case, ϵ_{∞} is set to 1.77 (water), and f is set to 0.04. In order to obtain higher coupling strength, the plasma frequency of the metal material needs to be higher and ϵ_{∞}^D needs to be smaller. The cases of two commonly used noble metal materials that support surface plasmon resonance, Au and Ag, are marked with golden and silver dots in Fig. 2. It can be seen that Ag is more suitable for designing plasmon-exciton coupling systems than Au under the same conditions. According to (2), $\Omega = 2\sqrt{((\omega_m - \tilde{\omega}_0)/2)^2 + G_1^2}$ corresponds to the spectrum splitting caused by plasmon-exciton coupling. At zero detuning ($\omega_m = \omega_0$), the theoretical condition required for observing Rabi splitting is $G_1^2 > (\Gamma_m - \Gamma_0)^2/16$. However, in order to observe clearly resolvable Rabi splitting in the experiment, the splitting given by $2[G_1^2 - (\Gamma_m - \Gamma_0)^2/16]^{1/2}$ must additionally exceed the value of the average line widths $(\Gamma_m + \Gamma_0)/2$, which leads to $G_1^2 \geq (\Gamma_m^2 + \Gamma_0^2)/8$. Combining this condition with (3), we can get requirements for material parameters to achieve strong coupling.

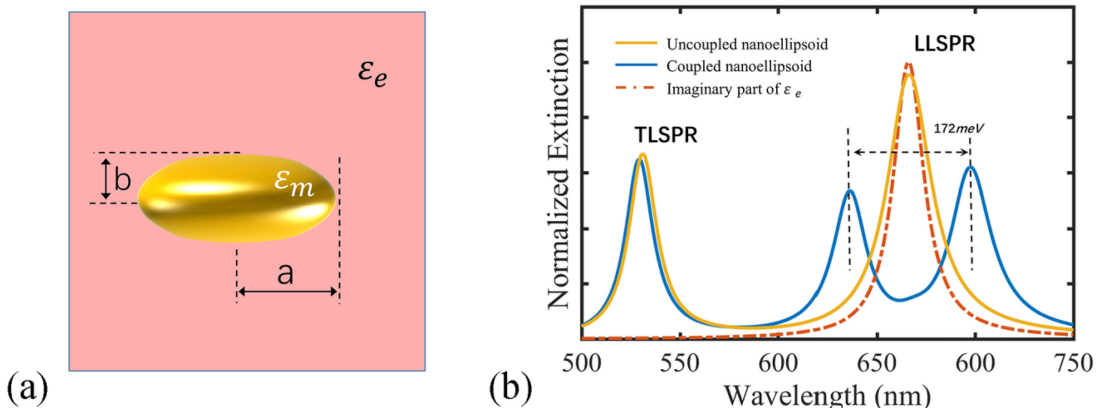


Fig. 3. (a) Schematic diagram of a metal nanoellipsoid surrounded by excitonic material. ϵ_m is the permittivity of the metal and ϵ_e is the permittivity of the excitonic material. (b) Extinction cross section of a Au nanoellipsoid in the coupled case and uncoupled case calculated from (4). f is set to 0.04 and ω_0 is set to 1.85 eV.

3. Metal Nanoellipsoid in Excitonic Medium

To further study the influence of geometric parameters on the interaction between the nanoparticles and the excitonic medium, we consider a more complex configuration, a metal nanoellipsoid in a uniform and infinite excitonic medium. Nanoellipsoid is one of the most general smooth particles of regular shape which can be solved analytically. Unlike nanosphere, nanoellipsoid have three different semi-axes (a, b, c). Their surface plasmon resonance characteristics strongly dependent on the three semi-axes, providing a convenient way to adjust the surface plasmon resonance. Nanorods, a class of practical nanoparticles often used in experiments, can be abstracted as nanoellipsoid with $a > b = c$, and their surface plasmon resonance can be controlled by the aspect ratio a/b . Fig. 3(a) shows the schematic diagram of the second configuration. The permittivity of the excitonic material and the metal are ϵ_e and ϵ_m . The major and minor semi-axes of the ellipsoid are a and b , respectively. The other semi-axis c is not shown in the diagram. By introducing the ellipsoid coordinate system, we can solve the corresponding Electromagnetic equations and obtain the polarizability of the nanoellipsoid (see the Supplementary Information, Section S2):

$$\alpha_{2_N} = 4\pi abc \frac{\epsilon_m - \epsilon_e}{3L_N(\epsilon_m - \epsilon_e) + 3\epsilon_e}. \quad (4)$$

$N = a, b, c$ corresponds to the three semi-axes of the ellipsoid. L_N is the geometrical factor (see the Supplementary Information, Section 2). When $b = c$, L_N is decided by the aspect ratio of nanoellipsoids. Substituting ϵ_m and ϵ_e into (4), we can obtain the extinction cross section of the small metal nanoellipsoid which is given by $C_{ext_2} \approx C_{abs} = k/m[\sum_{N=a,b,c} \alpha_{2_N}]$ (see the Supplementary Information, Section S5). Fig. 3(b) shows the extinction cross section of a Au nanoellipsoid with $a = 10$ nm, $b = c = 5$ nm in the coupled case and uncoupled case calculated from (4). The uncoupled nanoellipsoid has two resonance peaks corresponding to transverse localized surface plasmon resonance (TLSPR) and longitudinal localized surface plasmon resonance (LLSPR). The coupling strength between the LLSPR and excitons is stronger than that between the TLSPR and excitons which we will discuss later. Therefore, in the coupled case, we mainly consider the interaction between the LLSPR and the excitons. We set excitonic resonance energy as 1.85 eV to match the LLSPR and the parameter f as 0.04. The imaginary part of ϵ_e which corresponds to the absorption of excitonic material is shown with the red dotted line in Fig. 3(b). A large Rabi splitting about 172 meV arises in the extinction.

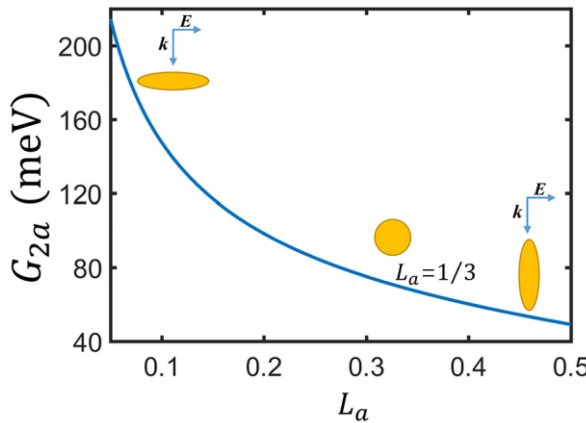


Fig. 4. Evolution of coupling constant G_{2a} vs the geometric factor L_a of the metal nanoellipsoid.

To achieve strong coupling, the LLSPR frequency has to be close to the exciton frequency. we make the assumption $\omega \approx \omega_0 \approx \omega_m$, the LLSPR frequency ω_m satisfies the following equation: $\text{Re}[L_a(\varepsilon_m - \varepsilon_e) + \varepsilon_e] = 0$ in the uncoupled case ($f = 0$), which leads to $\omega_0^2 \approx \omega_m^2 = (\omega_p^2 L_a)/(L_a \varepsilon_\infty^D + (1 - L_a)\varepsilon_\infty)$. The extinction cross section resulting from the a axis polarization can be reduced to $C_{ex_2} \propto \text{Im}[1/(\omega - \tilde{\omega}_{2-}) - 1/(\omega - \tilde{\omega}_{2+})]$ (see the Supplementary Information, Section S4). $\tilde{\omega}_{2\pm}$ are expressed as $\tilde{\omega}_{2\pm} = (\tilde{\omega}_m + \tilde{\omega}_0)/2 \pm \sqrt{(\tilde{\omega}_m - \tilde{\omega}_0/2)^2 + G_{2a}^2}$. The coupling constant G_{2a} can be written as:

$$G_{2a}^2 = \frac{f\omega_p^2}{4} \frac{L_a(1 - L_a)}{[L_a \varepsilon_\infty^D + (1 - L_a)\varepsilon_\infty]^2}. \quad (5)$$

According to (5), the coupling constant G_{2a} depends on the geometrical factor L_a . Fig. 4 shows the graph of the change of coupling constant with geometric factor. Here, different L_a actually corresponds to different coupling systems with the corresponding ω_0 and ω_m according to the assumption. As the geometric factor L_a increases, the coupling constant between a axis plasmonic resonance and excitons decreases. In order to correspond the geometrical factors to specific geometric shapes, we consider the nanoellipsoid as a prolate spheroid (cigar-shaped) which has one major axis and two equal minor axes. Then, $L_a < 1/3$ and $L_a > 1/3$ corresponds to the case where a axis is the major axis of the prolate spheroid and a axis is the minor axis of the prolate spheroid. When $L_a = 1/3$, the nanoellipsoid degenerates into a nanosphere. Comparing with the results in Fig. 4, we can conclude that at the same condition, the coupling strength between the LLSPR and excitons is stronger than that between the plasmon resonance of nanosphere and excitons, and the coupling strength between the plasmon resonance of nanosphere and excitons is stronger than that between the TLSPR and excitons. A larger aspect ratio of the nanoellipsoid gives a smaller geometric factor which leads to a stronger coupling strength.

Another important strong coupling phenomenon is the anticrossing behavior of the two energy branches with the detuning between plasmons and excitons changing. A common way to adjust the detuning is to change the geometric parameters of nanoparticles to adjust the plasmon resonance. Here, the evolution of the energy of the two branches in extinction spectra is obtained by changing the aspect ratio of the nanoellipsoid. The result is shown in Fig. 5. Aspect ratios of the nanoellipsoid are adjusted from 1 to 2.5. The resonant wavelength of the LLSPR has a nearly linear dependence on the aspect ratio, as the red dashed line depicts in Fig. 5. When the LSPPR energy crosses the absorption band of the excitons, typical of an anticrossing behavior is observed as a result of the strong plasmon-exciton coupling.

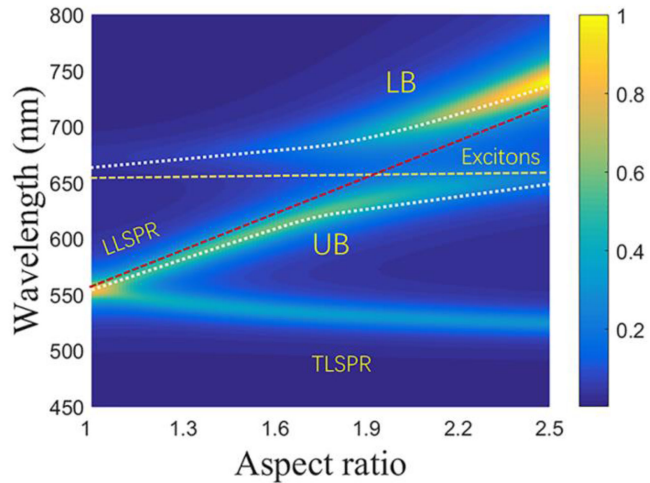


Fig. 5. Extinction spectra of the coupled nanoellipsoid with different aspect ratios.

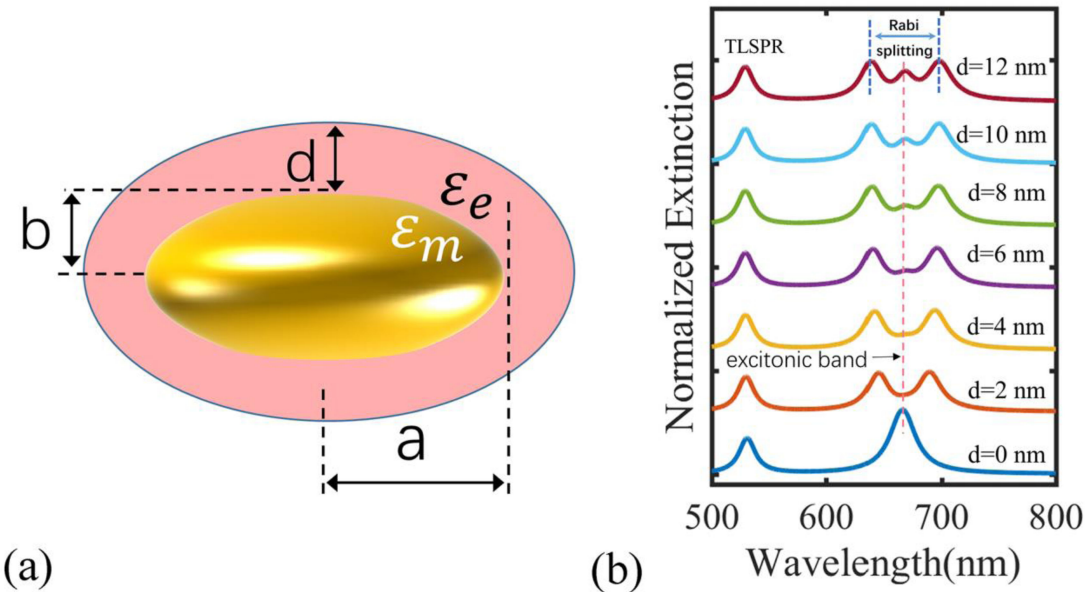


Fig. 6. (a) Schematic diagram of a metal nanoellipsoid coated with an excitonic layer. ϵ_b is the background permittivity (b) Extinction cross section of a Au nanoellipsoid coated with different thickness excitonic layers.

4. A Metal Nanoellipsoid Coated With an Excitonic Layer

In this section, we investigate a more practical situation: a metal nanoellipsoid homogeneously coated with an excitonic layer. Fig. 6(a) shows the schematic diagram of this configuration. The thickness of the excitonic layer is d . The major and minor semi-axes of the ellipsoid are a and b , respectively. The coated nanoellipsoid is placed in a background medium with permittivity ϵ_b . In experimental researches, rod-like nanoparticles coated with dye molecules are commonly used for plasmon-exciton coupling. [1], [12] For these cases, a metal nanoellipsoid homogeneously coated with an excitonic layer is a good analytic approximation. We can obtain the extinction cross section of the metal nanoellipsoid, which is given by $C_{ext_3} \approx C_{abs} = klm[\sum_{N=a,b,c} \alpha_{3_N}]$. The polarizability of the coated nanoellipsoid α_{3_N} is given in the Supplementary Information, Section S3. If we make the

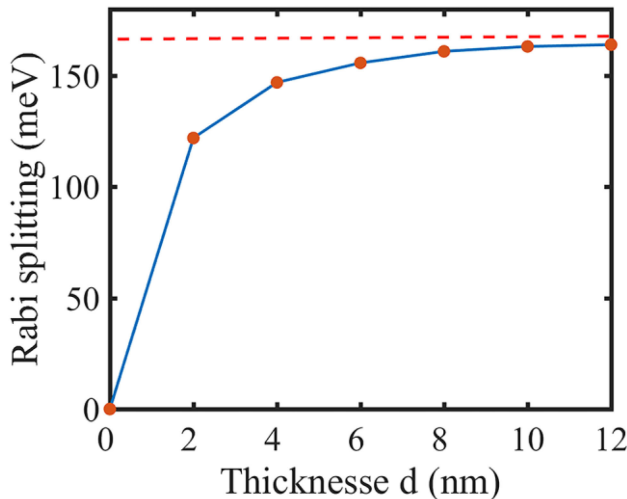


Fig. 7. Rabi splitting as a function of the excitonic layer thickness.

three semi-axes of the nanoellipsoid equal, this model will be transformed into a nanosphere coated with an excitonic layer. The extinction spectra of coated Au nanoellipsoids with different excitonic layer thickness are shown in Fig. 6(b). In the calculation, the parameters of the Au nanoellipsoid and the excitonic medium are the same as those set in Section 2. The three semi-axes of the metal nanoellipsoid are set as $a = 10$ nm, $b = c = 5$ nm. The excitonic layer thickness d varies from 0 nm to 12 nm, and the background permittivity ε_b is set to 2.5. Without the coating layer, the spectrum displays two resonance corresponding to the TLSR and LLSPR of the Au nanoellipsoid. After coating the nanoellipsoid with an excitonic layer, a Rabi doublet occurs in the extinction spectra and Rabi splitting increases with thickness. This phenomenon indicates that as the thickness of the exciton layer increases, more excitons participate in the interaction, resulting in a larger Rabi splitting. However, when the thickness increased to a certain extent, the change of Rabi splitting with the thickness gradually decreased. A new peak around the exciton absorption appears. It is due to the interaction between the dye molecules placed at a greater distance and the nanoparticle is weak, giving rise to the coexistence of weak and strong coupling.

Fig. 7 shows Rabi splitting as a function of the excitonic layer thickness. It shows that Rabi splitting increases with the thickness of the excitonic layer. When the excitonic layer thickness increases from 8 to 12 nm, Rabi splitting increases only slightly from 161 meV to 164 meV. This indicates that there is a Rabi splitting saturation phenomenon in the core-shell plexcitonic systems.

Finally, in order to verify the validity of our theory, we use a coated Au nanoellipsoid to reproduce the strong coupling phenomenon between the Au nanorods and J-aggregates in the experiment. The hybrid plexcitonic system consisting of nanorods and J-aggregates can be easily implemented experimentally and has been used to study strong coupling in the reference [12]. Fig. 8(a) shows the experimental extinction spectra of the uncoupled Au nanorods and the Au nanorods coated with excitonic material. The excitonic material we used here is J-aggregates of 56-dichloro-2-[[56-dichloro-1-ethyl-3-(4-sulfonylbutyl)-benzimidazol-2-ylidene]-propenyl]-1-ethyl-3-(4-sulfonylbutyl)-benzimidazolium hydroxide (TDBC) molecules. The absorption wavelength of J-aggregates (J-band) is located at 588 nm and the LLSPR wavelength of the uncoupled Au nanorods is about 590 nm. When the Au nanorods are coated with the J-aggregates, the extinction of the gold nanorods shows obvious Rabi splitting phenomenon, which proves that the strong coupling is achieved. This strong coupling phenomenon is theoretically reproduced in the Fig. 8(b) with a coated Au nanoellipsoid. In the calculation, the Au nanorods are abstracted as an Au ellipsoid and the three semi-axes of the Au nanoellipsoid are set as $a = 36$ nm, $b = c = 22$ nm, and the excitonic layer thickness d is set to 4 nm. The parameter f is set to 0.07 and the ω_0 is set to 2.1 eV (J-band).

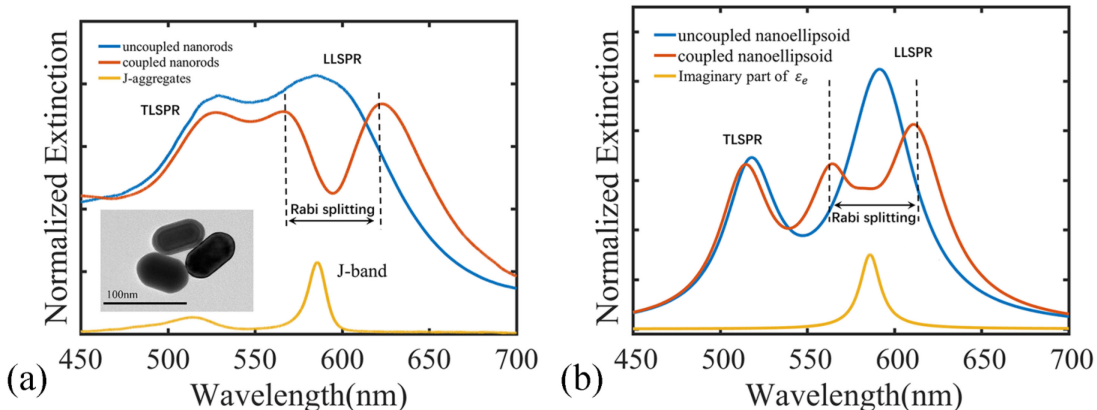


Fig. 8. (a) Experimental extinction spectra of the uncoupled Au nanorods, the Au nanorods coated with J-aggregates, and the J-aggregates. (Insert: transmission electron microscopy of the used Au nanorods) (b) Calculated extinction spectra of the uncoupled nanoellipsoid and the nanoellipsoid coated with an excitonic layer, and the imaginary part of ϵ_e .

ε_∞ is set to 2.5 and Γ_0 are set to 50 meV, respectively. The permittivity of Au is described by Drude model [32], and the metal loss was adjusted appropriately to fit the experimental results.

5. Conclusion

In conclusion, we present a semiclassical description of the interaction between localized surface plasmon resonances and excitons. Our approach is different from previous analytical studies of plasmon-exciton coupling, which have relied on purely phenomenological models of classical coupled oscillators. In these phenomenological models, the magnitude of the coupling strength is introduced as a free parameter not explicitly connected to the material or geometrical properties of the coupled system. We reveal the relations between the coupling strength and the material and geometrical parameters of several specific plexcitonic systems. Our results make a number of useful predictions for designing strongly coupled plasmon-exciton systems. In configuration 1 and 2, expressions for the plasmon-exciton coupling strengths of a metal nanosphere or nanoellipsoid in excitonic media are obtained, which are given by (3) and (5). It is concluded that Ag is more suitable for designing plasmon-exciton coupling systems than Au under the same conditions and the nanoellipsoid with a larger aspect ratio has stronger coupling strength when interacting with excitonic material. In configuration 3, we show that for a metal nanoellipsoid homogeneously coated with an excitonic layer, the thicker layer gives rise to a larger Rabi splitting. However, when the thickness increased to a certain extent, the molecules placed at a greater distance are only weakly coupled with the metal nanoellipsoid. Thus, there is a Rabi splitting saturation phenomenon in the core-shell plexcitonic systems. Our results provide a simple yet rigorous method for designing plexcitonic systems and have potential applications in quantum information processing, bio-sensing, and nanoscale optical devices.

References

- [1] R. Liu *et al.*, "Strong light-matter interactions in single open plasmonic nanocavities at the quantum optics limit," *Phys. Rev. Lett.*, vol. 118, no. 23, Jun. 2017, Art. no. 237401.
- [2] Y. Zakharko, A. Graf, and J. Zaumseil, "Plasmonic crystals for strong light-matter coupling in carbon nanotubes," *Nano. Lett.*, vol. 16, no. 10, pp. 6504–6510, Oct. 2016.
- [3] K. Santhosh, O. Bitton, L. Chuntonov, and G. Haran, "Vacuum rabi splitting in a plasmonic cavity at the single quantum emitter limit," *Nat. Commun.*, vol. 7, Jun. 2016, Art. no. 11823.

- [4] G. Zengin, M. Wersall, S. Nilsson, T. J. Antosiewicz, M. Kall, and T. Shegai, "Realizing strong light-matter interactions between single-nanoparticle plasmons and molecular excitons at ambient conditions," *Phys. Rev. Lett.*, vol. 114, no. 15, Apr. 2015, Art. no. 157401.
- [5] P. Xie *et al.*, "Enhanced coherent interaction between monolayer WS₂ and film-coupled nanocube open cavity with suppressed incoherent damping pathway," *Phys. Rev. B*, vol. 102, no. 11, 2020, Art. no. 115430.
- [6] J. J. Baumberg, J. Aizpurua, M. H. Mikkelsen, and D. R. Smith, "Extreme nanophotonics from ultrathin metallic gaps," *Nat Mater.*, vol. 18, no. 7, pp. 668–678, Jul. 2019.
- [7] D. Zheng, S. Zhang, Q. Deng, M. Kang, P. Nordlander, and H. Xu, "Manipulating coherent plasmon-exciton interaction in a single silver nanorod on monolayer WSe₂," *Nano. Lett.*, vol. 17, no. 6, pp. 3809–3814, Jun. 2017.
- [8] S. J. Ding *et al.*, "Strongly asymmetric spectroscopy in plasmon-exciton hybrid systems due to interference-induced energy repartitioning," *Phys. Rev. Lett.*, vol. 119, no. 17, Oct. 2017, Art. no. 177401.
- [9] P. Torma, and W. L. Barnes, "Strong coupling between surface plasmon polaritons and emitters: A review," *Rep. Prog. Phys.*, vol. 78, no. 1, Jan. 2015, Art. no. 013901.
- [10] N. T. Fofang, N. K. Grady, Z. Fan, A. O. Govorov, and N. J. Halas, "Plexciton dynamics: Exciton-plasmon coupling in a J-aggregate-Au nanoshell complex provides a mechanism for nonlinearity," *Nano. Lett.*, vol. 11, no. 4, Apr. 2011, Art. no. 1556.
- [11] W. Zhang, A. O. Govorov, and G. W. Bryant, "Semiconductor-metal nanoparticle molecules: Hybrid excitons and the nonlinear fano effect," *Phys. Rev. Lett.*, vol. 97, no. 14, Oct. 2006, Art. no. 146804.
- [12] D. Melnikau *et al.*, "Rabi splitting in photoluminescence spectra of hybrid systems of gold nanorods and J-aggregates," *J. Phys. Chem. Lett.*, vol. 7, no. 2, pp. 354–362, Jan. 2016.
- [13] F. Deng, H. Liu, L. Xu, S. Lan, and A. E. Miroshnichenko, "Strong exciton–plasmon coupling in a WS₂ monolayer on Au film hybrid structures mediated by liquid ga nanoparticles," *Laser Photon. Rev.*, vol. 14, no. 4, 2020, Art. no. 1900420.
- [14] E. M. Roller, C. Argyropoulos, A. Hogele, T. Liedl, and M. Pilo-Pais, "Plasmon-exciton coupling using DNA templates," *Nano. Lett.*, vol. 16, no. 9, Sep. 2016, Art. no. 5962.
- [15] T. K. Hakala *et al.*, "Bose–Einstein condensation in a plasmonic lattice," *Nature Phys.*, vol. 14, no. 7, pp. 739–744, 2018.
- [16] T. K. Hakala *et al.*, "Lasing in dark and bright modes of a finite-sized plasmonic lattice," *Nat. Commun.*, vol. 8, Jan. 2017, Art. no. 13687.
- [17] M. J. Holmes, K. Choi, S. Kako, M. Arita, and Y. Arakawa, "Room-temperature triggered single photon emission from a III-Nitride site-controlled nanowire quantum dot," *Nano. Lett.*, vol. 14, no. 2, pp. 982–986, 2014.
- [18] H. Shan *et al.*, "Direct observation of ultrafast plasmonic hot electron transfer in the strong coupling regime," *Light Sci. Appl.*, vol. 8, pp. 9, 2019, Art. no. 9.
- [19] T. Schwartz, J. A. Hutchison, C. Genet, and T. W. Ebbesen, "Reversible switching of ultrastrong light-molecule coupling," *Phys. Rev. Lett.*, vol. 106, no. 19, May 2011, Art. no. 196405.
- [20] M. Wersall, J. Cuadra, T. J. Antosiewicz, S. Balci, and T. Shegai, "Observation of mode splitting in photoluminescence of individual plasmonic nanoparticles strongly coupled to molecular excitons," *Nano. Lett.*, vol. 17, no. 1, pp. 551–558, Jan. 2017.
- [21] X. Chen *et al.*, "Mode modification of plasmonic gap resonances induced by strong coupling with molecular excitons," *Nano. Lett.*, vol. 17, no. 5, pp. 3246–3251, May 2017.
- [22] A. E. Schlather, N. Large, A. S. Urban, P. Nordlander, and N. J. Halas, "Near-field mediated plexcitonic coupling and giant rabi splitting in individual metallic dimers," *Nano. Lett.*, vol. 13, no. 7, Jul 2013, Art. no. 3281.
- [23] O. Bitton *et al.*, "Vacuum rabi splitting of a dark plasmonic cavity mode revealed by fast electrons," *Nat. Commun.*, vol. 11, no. 1, pp. 487, Jan 2020, Art. no. 487.
- [24] J. Qin *et al.*, "Revealing strong plasmon-exciton coupling between nanogap resonators and two-dimensional semiconductors at ambient conditions," *Phys. Rev. Lett.*, vol. 124, no. 6, Feb 2020, Art. no. 063902.
- [25] H. Groß, J. M. Hamm, T. Tufarelli, O. Hess, and B. Hecht, "Near-field strong coupling of single quantum dots," *Sci. Adv.*, vol. 4, no. 3, 2018, Art. no. eaar4906.
- [26] R. Chikkaraddy *et al.*, "Single-molecule strong coupling at room temperature in plasmonic nanocavities," *Nature*, vol. 535, no. 7610, pp. 127–130, Jul. 2016.
- [27] S. Balci, B. Kucukoz, O. Balci, A. Karatay, C. Kocabas, and G. Yaglioglu, "Tunable plexcitonic nanoparticles: A model system for studying plasmon–exciton interaction from the weak to the ultrastrong coupling regime," *ACS Photon.*, vol. 3, no. 11, pp. 2010–2016, 2016.
- [28] R. K. Yadav *et al.*, "Room temperature weak-to-strong coupling and the emergence of collective emission from quantum dots coupled to plasmonic arrays," *ACS Nano.*, vol. 14, no. 6, pp. 7347–7357, Jun. 2020.
- [29] F. Wu *et al.*, "Plexcitonic optical chirality: Strong exciton–plasmon coupling in chiral J-aggregate-metal nanoparticle complexes," *ACS Nano.*, vol. 15, no. 2, pp. 2292–2300, Dec. 2020.
- [30] J. A. Faucheaux, J. Fu, and P. K. Jain, "Unified theoretical framework for realizing diverse regimes of strong coupling between plasmons and electronic transitions," *J. Phys. Chem. C*, vol. 118, no. 5, pp. 2710–2717, 2014.
- [31] S. K. G. Xiaohua Wu, and M. Pelton, "Quantum-dot-induced transparency in a nanoscale plasmonic resonator," *Opt. Exp.*, vol. 18, no. 23, pp. 23633–23645, 2010.
- [32] A. Vial, A.-S. Grimalt, D. Macías, D. Barchiesi, and M. L. de la Chapelle, "Improved analytical fit of gold dispersion: Application to the modeling of extinction spectra with a finite-difference time-domain method," *Phys. Rev. B*, vol. 71, no. 8, 2005, Art. no. 085416.
- [33] G. Zengin, G. Johansson, P. Johansson, T. J. Antosiewicz, M. Kall, and T. Shegai, "Approaching the strong coupling limit in single plasmonic nanorods interacting with J-aggregates," *Sci. Rep.*, vol. 3, Oct. 2013, Art. no. 3074.